Hydrol. Earth Syst. Sci. Discuss., 6, 7001–7024, 2009
www.hydrol-earth-syst-sci-discuss.net/6/7001/2009/

Hydrology and Earth System Sciences Discussions

This discussion paper is/has been under review for the journal Hydrology and Earth System Sciences (HESS). Please refer to the corresponding final paper in HESS if available.

Accurate LAI retrieval method based on PROBA/CHRIS data

W. Fan[1], X. Xu[1], X. Liu[2], B. Yan[1], and Y. Cui[1]

[1]Institute of Remote Sensing and GIS, Peking University, Beijing, China
[2]International Institute for Earth System Science, Nanjing University, Nanjing, China

Received: 30 September 2009 – Accepted: 29 October 2009 – Published: 12 November 2009

Correspondence to: W. Fan (fanwj@pku.edu.cn)

Published by Copernicus Publications on behalf of the European Geosciences Union.

Abstract

Leaf area index (LAI) is one of the key structural variables in terrestrial vegetation ecosystems. Remote sensing offers a chance to derive LAI in regional scales accurately. Variations of background, atmospheric conditions and the anisotropy of canopy reflectance are three factors that can strongly restrain the accuracy of retrieved LAI. Based on the hybrid canopy reflectance model, a new hyperspectral directional second derivative method (DSD) is proposed in this paper. This method can estimate LAI accurately through analyzing the canopy anisotropy. The effect of the background can also be effectively removed. So the inversion precision and the dynamic range can be improved remarkably, which has been proved by numerical simulations. As the derivative method is very sensitive to the random noise, we put forward an innovative filtering approach, by which the data can be de-noised in spectral and spatial dimensions synchronously. It shows that the filtering method can remove the random noise effectively; therefore, the method can be performed to the remotely sensed hyperspectral image. The study region is situated in Zhangye, Gansu Province, China; the hyperspectral and multi-angular image of the study region has been acquired from Compact High-Resolution Imaging Spectrometer/Project for On-Board Autonomy (CHRIS/PROBA), on 4 and 14 June 2008. After the pre-processing procedures, the DSD method was applied, and the retrieve LAI was validated by the ground truth of 11 sites. It shows that by applying innovative filtering method, the new LAI inversion method is accurate and effective.

1 Introduction

Leaf area index (LAI) is one of the important geometrical structure parameters in terrestrial vegetation ecosystems. Accurate LAI retrieval is always a key task of remote sensing applications, and is also the precondition of the crop yield estimation, vegetative evapotranspiration calculation and the energy exchange evaluation of terrestrial

vegetation (Badhwar et al., 1986; Townshend et al., 1988; Baret et al., 1991; Wood et al., 1993; Bonan, 1995; Bicheron et al., 1999; Buermann et al., 2001; Kamalesh et al., 2008). In general, there are three categories of LAI retrieval method. The first category is experiential inversion method based on Vegetation Index (VI), such as retrieving LAI according to the correlation between NDVI and LAI (Turner, 1999; Brown et al., 2000; Haboudane et al., 2004; Wang et al., 2005). Although simple and widely used, its accuracy is very low, and VI is easy to be saturated. The second category can be called the reflectance model inversion method, by which the anisotropic effect caused by sun-object-sensor geometry can be removed, but the effect caused by background variations cannot be avoided, especially within mixed pixels. The complex background embarrasses accurate LAI retrieval (Li et al., 1986; Nilson et al., 1989; Chen et al., 1997; Xu, 2005). According to the fact that the hyperspectral second derivative was founded at the end of 1980s and that it can remove the effect of soil background effectively, the hyperspectral derivative method was established to retrieve LAI (Pu et al., 2000). Since the method is sensitive to noise even if the canopy anisotropy is neglected, it is difficult to be used operationally. The proper filtering method, which can remove the effect of the canopy anisotropy and background reflectance variations, becomes the key factor of LAI retrieval.

On 22 October 2001, PROBA (Project On-Board Autonomy) was launched as a technology demonstrator within ESA's General Support Technology Programme. CHRIS (Compact High Resolution Imaging Spectrometer), the prime instrument of the PROBA mission, is hyperspectral whose objective is data collection of BRDF (Bidirectional Reflectance Distribution Function) for a better understanding of the spectral reflectance. CHRIS acquires a set of images with five view angles (−55°, −36°, 0°, 36°and 55°) of each target during each acquisition sequence in 2.5 min (Verrelst et al., 2007; Kamalesh et al., 2008; CHRIS/PROBA Website), and a total of 62 band images in visible-near infrared regions from 400 nm to 1050 nm. The new hyperspectral sensor offers a new opportunity to improve the inversion accuracy of LAI effectively. The main objective of this paper is to establish a useful method that can best estimate LAI by multi-

angular hyperspectral data, because it can restrain the effect of background variations and the canopy anisotropic reflectance.

2 The model

Supposing the height of canopy is H, there are four components within the view field of sensor, which are illuminated ground and canopy, as well as shadowed ground and canopy; K_g, K_c, K_z, K_t represent the area ratios of the four parts, respectively. Reflectance of targets can be described as $\rho = \rho^1 + \rho^m$, where ρ^1 stands for the reflectance contributed by the single scattering and ρ^m multiple scattering (Li et al., 1986; Nilson et al., 1989; Nilson, 1991; Chen, 1997). ρ^1 describes the anisotropic characteristics of the object, and according to the geometric model it can be expressed as (Xu, 2009):

$$\rho^1 = \rho_g \left\{ e^{-\lambda_0 \left[\frac{G_S}{\mu_0} + \frac{G_V}{\mu_V} - \frac{G_V}{\mu_V}\cdot\Gamma(\phi)\right]\mathrm{LAI}} + \left[e^{-\lambda_0 \frac{G_V}{\mu_V}\cdot\mathrm{LAI}} - e^{-\lambda_0 \left[\frac{G_S}{\mu_0} + \frac{G_V}{\mu_V} - \frac{G_V}{\mu_V}\cdot\Gamma(\phi)\right]\mathrm{LAI}} \right] \frac{E_d}{\mu_0 F_0 + E_d} \right\} + \rho_V \left\{ \left(1 - e^{-\lambda_0 \frac{G_V}{\mu_V}\cdot\mathrm{LAI}\cdot\Gamma(\phi)}\right) + \left[e^{-\lambda_0 \frac{G_V}{\mu_V}\cdot\mathrm{LAI}\cdot\Gamma(\phi)} - e^{-\lambda_0 \frac{G_V}{\mu_V}\cdot\mathrm{LAI}} \right] \frac{E_d}{\mu_0 F_0 + E_d} \right\} \quad (1)$$

Here ρ_g and ρ_v are the hemispherical albedos of the soil background and the leaf, G_v and G_s mean the G function of the view direction and the solar direction, respectively (Xu, 2005); $\mu_v = \cos\theta_v$, $\mu_0 = \cos\theta_0$, θ_v and θ_0 are the viewing zenith angle and the solar zenith angle, respectively. Nilson parameter (λ_0) is used to describe the clumping effect of foliage (Nilson et al., 1989). $\Gamma(\phi)$ is an empirical function used to describe the hot spot effect. ϕ is the angle between light and viewing directions. $\Gamma(0)=1$, $\Gamma(\pi)=0$, when $0<\phi\leq\pi$, and $\Gamma(\phi) = e^{-\frac{\phi}{\pi-\phi}}$. $\mu_0 F_0$ is the direct irradiance of the sun, and E_d is the diffuse irradiance of atmosphere; the contribution of multi-scattering can be expressed by Hapke model (Hapke, 1981, 1986).

In order to evaluate the hybrid model, we use the field test data measured in Shunyi District, Beijing 2001, which was covered by winter wheat (Wang et al., 2006). Mea-

HESSD
6, 7001–7024, 2009

surements were carried out using ASD with a spectral range from 400 nm to 2500 nm. For the same points, several measurements were taken in different viewing directions along the principle plane, varying from −40° (backward) to 40° (forward) at an interval of 5°. The bi-directional reflectance spectrums simulated by the model are almost consonant with the measured spectrums (Fig. 1).

3 The methodology of directional second derivative

When $\rho''_v \gg \rho''_g$, Eq. (1) can be written as:

$$\rho'' = \rho''_1 + \rho''_m \approx \rho''_v \left(1 - e^{-\lambda_0 \frac{G_V}{\mu_V} \mathrm{LAI}\Gamma(\phi)}\right) + \frac{E_d}{\mu_0 F_0 + E_d} \rho''_v \left(e^{-\lambda_0 \frac{G_V}{\mu_V} \mathrm{LAI}\Gamma(\phi)} - e^{-\lambda_0 \frac{G_V}{\mu_V} \mathrm{LAI}}\right) + \rho''_m \quad (2)$$

ρ'', ρ''_v and ρ''_g are the second derivative of wavelength for the object, the leaf and the soil spectrum, respectively. According to Eq. (2) ρ'' is independent of the soil spectrum.

3.1 Band choice

Comparing the second derivative spectra simulated by the new hybrid canopy reflectance model with the second derivative spectra measured in the different background (Fig. 2), $\rho''_v \gg \rho''_g$ can be satisfied within bands of 0.68–0.71μm and 0.73–0.75μm, not only for the soil background but also for the water body, concrete and so on. So the hyperspectral second derivative method can remove the effect of background effectively. At the same time Fig. 3 shows that the multiple scattering can be ignored within 0.68–0.71 μm, thus it is the best band area choice.

HESSD
6, 7001–7024, 2009

3.2 Inversion formula

As mentioned earlier, within 0.68–0.71μm, the multiple scattering can be neglected completely, so Eq. (2) can be transformed; suppose $X=\frac{\rho''}{\rho''_v}$, then

$$X = 1 - \left[1 - \frac{E_d}{\mu_0 F_0 + E_d}\left(1 - e^{-\lambda_0 \frac{G_v}{\mu_v}(1-\Gamma(\phi))\mathrm{LAI}}\right)\right] e^{-\lambda_0 \frac{G_v}{\mu_v}\mathrm{LAI}\Gamma(\phi)} \quad (3)$$

Equation (3) is the directional second derivative (DSD) inversion formula of LAI. When ϕ=0, $\Gamma(0)$=1 that is the hotspot direction; if $b=\lambda_0\frac{G_v}{\mu_v}$ we have

$$X = 1 - e^{-\mathrm{bLAI}} \quad (4)$$

Equation (4) shows the relationship between the second derivative and LAI, as the target is supposed to be lambertian. In fact, the vegetation-soil system is non-isotropic, and the relationship between the second derivative and LAI changes with the solar and view angles. It is just the difference between Eqs. (3) and (4). The range of G_v is 0.3~0.8, and λ_0 can be gained as the priori knowledge. $0<\lambda_0<1$, θ_v is known, and $\theta_v<60^\circ$. So $\Gamma(\phi)$ is the only parameter that can dramatically affect the relationship between X and LAI.

Figure 4 shows the relationship between X and LAI as $\Gamma(\phi)$ changes. It can also be found the sensitivity of DSD method is very high, and that the dynamic range of the method is also large. The optimal view angle for LAI inversion is near the hot spot. When the view angle is near the cold spot, X can quickly saturate when LAI equals to 3, so the direction is not suitable for LAI retrieval. Numerical simulations also show that the inversion error can be less than 5% in the hot spot direction when LAI is larger than 0.5, even when 15% random errors are added (Fig. 5). The effective range of the method is LAI>0.5. When the LAI is very low, the information of vegetation is also very low. Therefore, it is impossible to retrieve LAI accurately.

HESSD
6, 7001–7024, 2009

4 The innovative filtering approach

As mentioned before, the DSD method is very sensitive to noise, so it is necessary to conduct pre-procedure to remove the effect of noise. An innovation de-noising method is proposed that can filter the noise in both spectral dimension and spatial dimension. Firstly, the Minimum Noise Fraction (MNF) transform is used in the spatial dimension, and then the Fast Fourier Transform (FFT) in spectral dimension is adopted.

As far as the maize and the wheat canopy spectrum in the study area are concerned, the spectra variation in the visible-near infrared band (400–900 nm) are mainly caused by LAI and Chlorophyll concentration of the leaf, according to related study (Liu et al., 2000; Pu et al., 1997, 2000). The variation of canopy spectra through the Fourier transform caused by LAI and the Chlorophyll concentration can be found only within the low frequency domain, much lower than the noise frequency, so a threshold can be found in the frequency domain to distinguish the useful signal and noise. In this case, noise in the hyperspectral image can be removed by the low-pass filter. The Butterworth low-pass filter is chosen, but the threshold of the low-pass filter function should be determined first. In order to determine frequency ranges caused by the variation of LAI and Chlorophyll concentration, the spectra simulated by PROSAIL model are adopted as the benchmark without the noise. The Fourier Transform of the canopy spectrum is analyzed to choose the threshold for Butterworth low-pass filter. Because mode 3 of CHRIS only acquired 18 bands, the spectrum is linearly interpolated to 180 bands first. By comparing the simulated reflectance with image samples in the frequency domain, the minimal value of Butterworth low-pass filter is given as 0.01283; frequency higher than it can be recognized and wiped out.

The result using the FFT smoothing is shown in Fig. 6. By the two-step de-noising method, the result is more reasonable. The CHRIS images at 0° angle before and after filtering in the study region are shown in Fig. 7.

5 Study region and dataset

5.1 Study region

The study region is an oasis, situated in Zhangye City, in the middle reach of the Heihe River Basin, the second largest inland river basin (37° 45′~42° 40′ N, 97° 42′~102° 04′ E) in China. It is one of the most extremely arid areas of the country. The type and distribution of landscapes and the Plant communities in the region can be found in website http://heihe.westgis.ac.cn/. The crops sowed in the oasis are mainly maize, wheat, barley and benne, and the growth of these crops always requires irrigation. The "Watershed Allied Telemetry Experiment Research (WATER)" remote sensing experiment was carried out in the Heihe River Basin, 2008. Our field experiment is one part of WATER.

5.2 Pre-processing of spaceborne CHRIS image

The image of CHRIS was acquired on 4 June 2008, which is the 1A product. Mode 3 for land studies results in a spatial resolution of approximately 17 m at nadir and a band set consisting of 18 bands. At first, the HDFCLEAN software was used to get rid of the stripes in the image. The radiation of the image was corrected using the gain and bias provided by the CHRIS programme. The geometric correction was processed using 1:10 000 scale topographic maps. The geocorrection root mean squared error (RMSE) of 5 angles' images is all less than one pixel. As the pixel sizes in 5 view angles are different, the resolutions of 5 images are over an average of 51 m to remove the effect of view angles. Four images of the study region were intercepted to retrieve LAI (Fig. 8).

Atmospheric correction of the CHRIS radiance data products is performed to obtain the surface reflectance using the atmospheric sounding data and ACORN 1.5 mode, which is specialized atmospheric correction software for the high-spectral image. ACORN is capable of processing data from tilted sensors by accounting for varying path lengths through the atmosphere and varying transmittance. Atmospheric cor-

rection results in the retrieval of HDRF (Hemispherical Directional Reflectance Factor) data sets for the various CHRIS view angles. Figure 9 shows the spectrums before and after the atmospheric processing.

6 Field measurements and validation

Ground truth data were collected in a maize and wheat field, the same as prior knowledge, G_v=0.6, λ_0=0.6 in the maize canopy, and G_v=0.1, λ_0=0.97 in the wheat canopy. Ground data collection included spectra radiometric measurements using a FieldSpecPro FR, LAI measurements using a LI-COR LAI-2000 Plant Canopy Analyzer, harvesting method and LI-COR LAI 3000 area meter, as well as leaf water and chlorophyll content in the laboratory. The reflectance of 706 nm band was used to calculate the directional second derivative, θ_s=25°, φ_s=137.00° when CHRIS transited the study area on 4 and 24 June 2008. Firstly the sowing area of maize and wheat was classified, and LAI was retrieved from CHRIS data of 5 angles, based on the least square method. The retrieved LAI is shown in Fig. 10. In order to evaluate the LAI retrieval performance, the estimated LAI (Fig. 10) has been compared with the LAI retrieved by NDVI method according to the field measurements (Fig. 11). It can be found from the two figures the inversion LAI using DSD method is more reasonable. Obvious changes in gradient are shown in Fig. 10. The error (RMSE) has been analyzed to quantify the agreement between actual LAI in 11 sites and estimated values (Table 1).

7 Results and discussion

In this paper, the relationship between the second derivative of different view angles and LAI was established based on the new hybrid canopy reflectance model. Numerical simulation shows that, this method can not only eliminate the effect of background and the anisotropy of canopy reflectance, but also improve the dynamic range and inversion accuracy.

As the DSD method is sensitive to noise, the innovation de-noising method is proposed, which can help to get rid of the noise in the spatial dimension and the spectral dimension. And the threshold of the low-pass filter function is determined according to the spectra simulated by PROSAIL model with the changes in LAI and chlorophyll concentration. The study shows that the new filtering method can eliminate the random noise of the CHRIS image.

In order to validate the DSD method, Zhangye, Gansu Province was chosen as the study region. The LAI was retrieved using multi-angular and hyperspectral CHRIS images on 4 June 2008. In order to evaluate the LAI retrieval performance, the estimated LAI using DSD method was compared with the LAI retrieved using NDVI method according to the field measurements and the ground truth. It shows that the DSD method can inverse LAI accurately, when applying the innovation de-noising method.

If the sensor owns more than 3 view angles, the G function, λ_0 and LAI can be inversed simultaneously, and the requirement of priori knowledge can be reduced, but the inversion accuracy will be influenced. This will be the next step of our effort.

Acknowledgements. This paper is supported by the Special Funds for Major State Basic Research Project (Grant No. 2007CB714402), the National Natural Science Foundation of China (Grant No. 40871186, Grant No. 40734025 and Grant No. 40401036) and the National High Technology Research and Development Program of China (Grant No. 2009AA12Z143).

References

Badhwar, G. D., MacDonald, R. B., and Metha, N. C.: Satellite-derived leaf-area-index and vegetation maps as input to global carbon cycle models – a hierarchical approach, Int. J. Remote Sens., 7, 265–281, 1986.

Baret, F. and Guyot, G.: Potentials and limits of vegetation indices for LAI and APAR assessment, Remote Sens. Environ., 35, 161–173, 1991.

Bicheron, P. and Leroy, M.: A method of biophysical parameter retrieval at global scale by inversion of a vegetation reflectance model, Remote Sens. Environ., 67, 251–266, 1999.

Bonan, G. B.: Land-atmosphere interactions for climate system models: coupling biophysical, biogeochemical, and ecosystem dynamical processes, Remote Sens. Environ., 51, 57–73, 1995.
Brown, L., Chen, J. M., Leblanc, S. G., and Cihlar, J. A.: Shortwave infrared modification to the simple ration for LAI retrieval in boreal forest: an image and model analysis, Remote Sens. Environ., 71, 16–25, 2000.
Buermann, W., Dong, J., Zeng, X., Myneni, R. B., and Dickinson, R. E.: Evaluation of the utility of satellite-based vegetation leaf area index data for climate simulations, J. Climate, 14(17), 3536–3550, 2001.
Chen, J. M. and Leblanc, S.: A 4-scale bidirectional reflection model based on canopy architecture, IEEE T. Geosci. Remote S., 35, 1316–1337, 1997.
CHRIS/PROBA Website: http://earth.esa.int/missions/thirdpartymission/proba.html, access: 30 October 2009.
Haboudane, D., Miller, J. R., Pattey, E., Zarco-Tejada, P. J., and Strachan, I. B.: Hyperspectral vegetation indices and novel algorithm for predicting green LAI of crop canopies: modeling and validation in the context of precision agriculture, Remote Sens. Environ., 90, 337–352, 2004.
Hapke, B.: Bidirectional reflectance spectroscopy: 1. Theory, J. Geophys. Res., 86, 3039–3054, 1981.
Hapke, B.: Bi-directional reflectance spectroscopy: 4. The extinction coefficient and the opposition effect, Icarus, 67, 264–280, 1986.
Kamalesh, V. L., Luckman, A., Grey, W. M. F., et al.: Estimation of leaf area index from PROBA/CHRIS hyperspectral, multi-angular data, in: Proceedings of the Remote Sensing and Photogrammetry Society Conference, 15–17 September 2008.
Li, X. W. and Strahler, A. H.: Geometric-optical bidirectional reflectance modeling of a coniferous forest canopy, IEEE T. Geosci. Remote S., 24, 906–919, 1986.
Liu, W. D., Xing, Y. Q., Zheng, L. F., and Tong, Q. X.: Relationships between Rice LAI, CH.D and hyperspectral data, J. Remote Sens., 4(4), 279–283, 2000.
Townshend, J. R. G. and Justice, C. O.: Selecting the spatial resolution of satellite sensors required for global monitoring of land transformations, Int. J. Remote Sens., 9, 187–236, 1988.
Turner, D. P., Cohen, W. B., Kennedy, R. E., Fassnacht, K. S., and Briggs, J. M.: Relationships between leaf area index and Landsat TM spectral vegetation indices across three temperate

zone sites, Remote Sens. Environ., 70, 52–68, 1999.
Nilson, T. and Kuusk, A.: A reflectance model for the homogeneous plant canopy and its inversion, Remote Sens. Environ., 27, 157–167, 1989.
Nilson, T.: Approximate analytical methods for calculating the reflection functions of leaf canopies in remote sensing applications, in: Photon-vegetation Interactions: applications in optical remote sensing and plant physiology, edited by: Myneni, R. B. and Ross, J., Springer Verlag, New York, 162–189, 1991.
Pu, R. and Gong, P.: Relationships between forest biochemical concentrations and CASI data along the Oregon transect, J. Remote Sens., 1(2), 115–123, 1997.
Pu, R. and Gong, P.: Hyperspectral Remote Sensing and Its Applications, Higher Education Press, Beijing, China, 2000.
Verrelst, J., Schaepman, M. E., Koetz, B., and Kneubuehler, M.: Angular sensitivity analysis of vegetation indices derived from CHRIS/PROBA data, Remote Sens. Environ., 112(5), 2341–2353, 2007.
Wang, J. D. and Liu, S. H.: The Remote Sensing Standardized Spectral Database and Non-spectral Parameters of Typical Objects in China, Center of Remote Sensing and GIS, Beijing Normal University, 2006.
Wang, Q., Adiku, S., Tenhunen, J., and Granier, A.: On the relationship of NDVI with leaf area index in a deciduous forest site, Remote Sens. Environ., 94, 245–255, 2005.
Wood, E. F. and Lakshmi, V.: Scaling water and energy fluxes in climate systems: three land-atmospheric modeling experiments. J. Climate, 6, 439–857, 1993.
Xu, X. R.: Vegetation remote sensing models, in: Physics of remote sensing, edited by: Xu, X. R., Peking University Press, Beijing, China, 47–49, 2005.
Xu, X. R., Fan, W. J., and Tao, X.: The spatial scaling effect of continuous canopy leaves area index retrieved by remote sensing, Sci. China Ser. D, 52, 393–401, 2009.

Table 1. Error analysis of retrieval results using CHRIS image.

	The average error	The maximum error	The minimum error	Standard deviation of errors
NDVI method	0.710	2.082	0.227	0.405
DSD method	−0.075	0.21	0.005	0.118

HESSD
6, 7001–7024, 2009

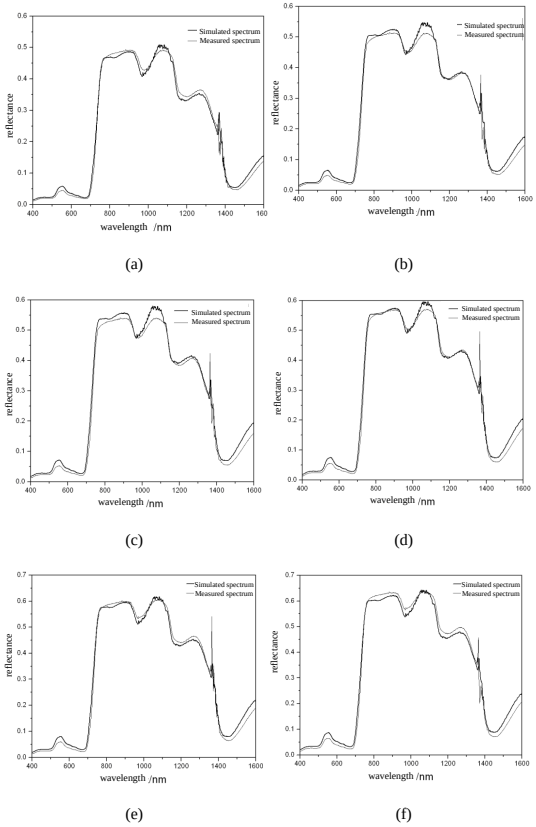

Fig. 1. The comparisons between simulated reflectance and measured reflectance (θ_s=36°, ϕ=44°, LAI=4.25) **(a)** θ_v=10°; **(b)** θ_v=20°; **(c)** θ_v=30°; **(d)** θ_v=40°; **(e)** θ_v=50°; **(f)** θ_v=60°.

HESSD
6, 7001–7024, 2009

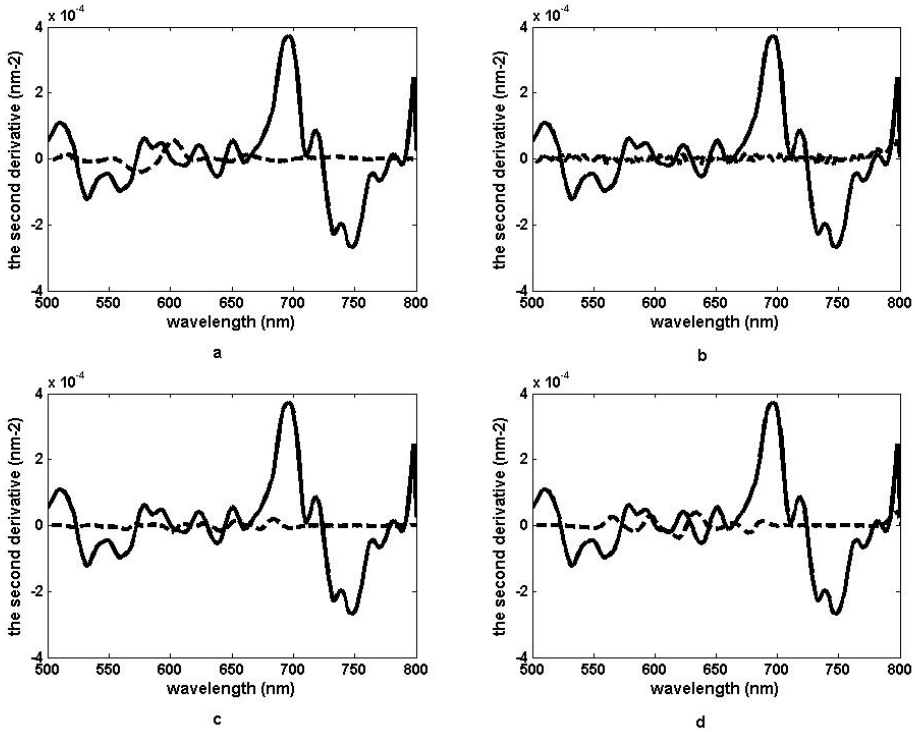

Fig. 2. Comparison of second derivative of leaf spectrum and different background spectra.

HESSD
6, 7001–7024, 2009

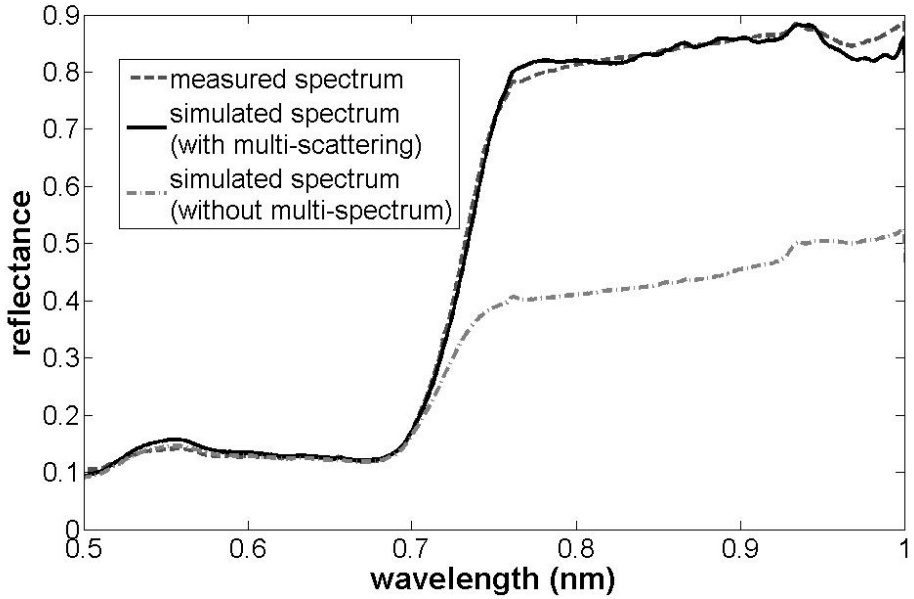

Fig. 3. Impacts of multi-scattering on reflectance spectra.

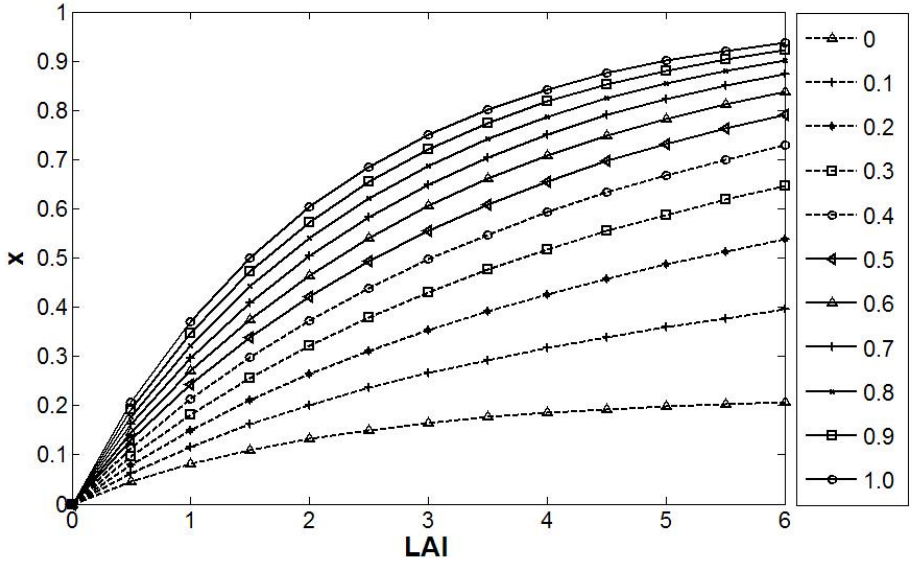

Fig. 4. Relationship between LAI and X at different values of $\Gamma(0)$.

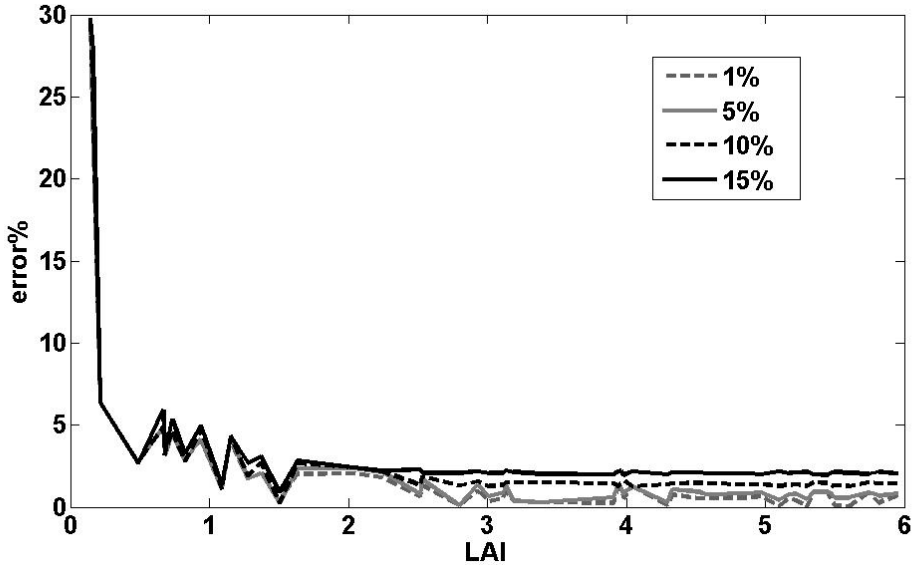

Fig. 5. The inversion error of the method in numerical simulation.

HESSD
6, 7001–7024, 2009

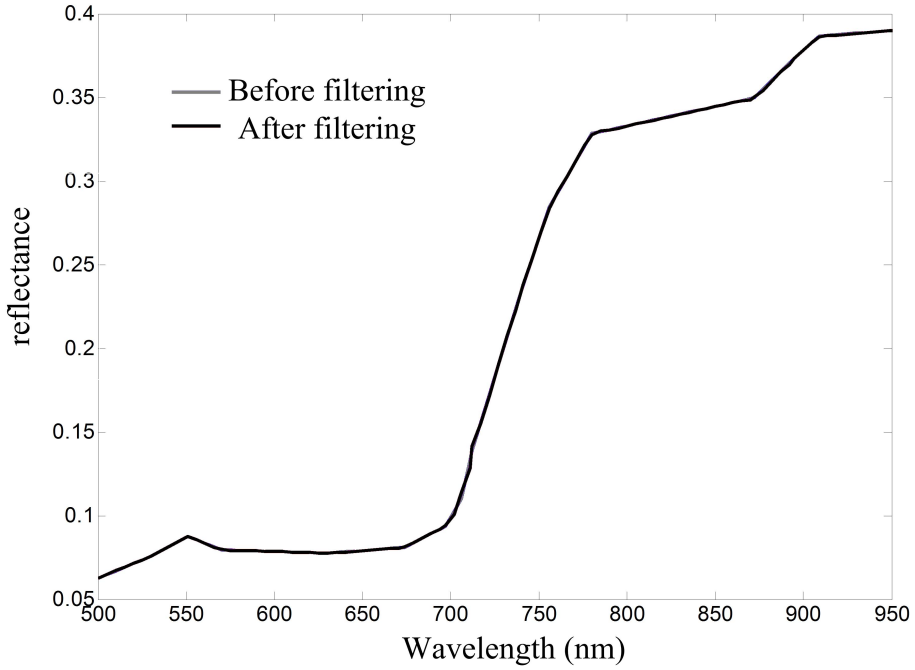

Fig. 6. Comparison of canopy spectra on CHRIS image before and after filtered using the two-step denoising method.

HESSD
6, 7001–7024, 2009

(a) before (b) after

Fig. 7. Comparison of CHRIS 0° images of the study area before and after filtered.

HESSD
6, 7001–7024, 2009

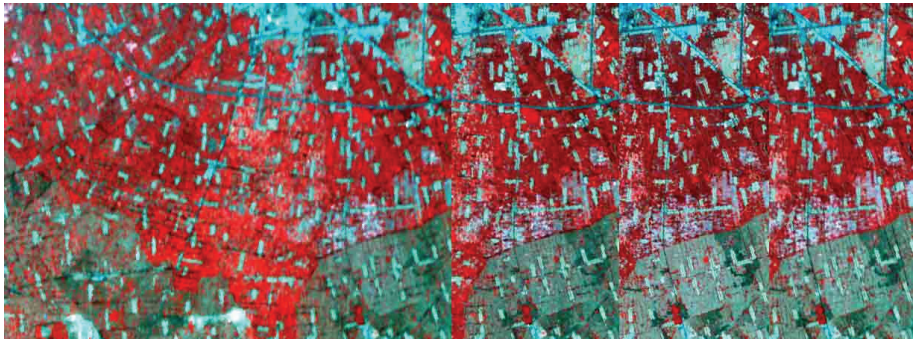

Fig. 8. CHRIS images covering the study area of four view angles after geometric correction (the view angle from left to right is 55°, 36°, 0°, −36°, respectively).

HESSD

6, 7001–7024, 2009

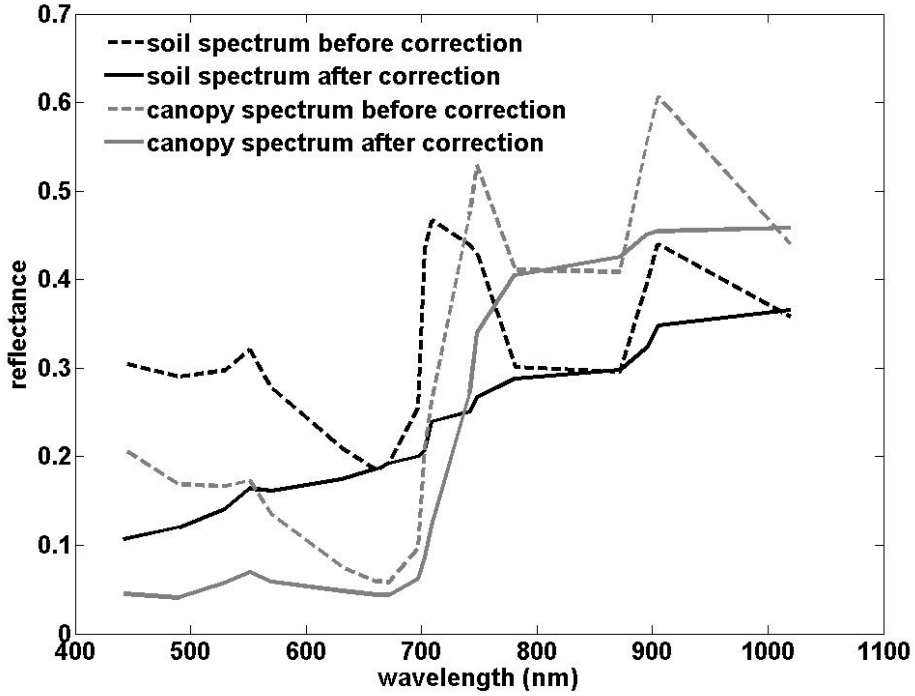

Fig. 9. Soil and canopy spectra on CHRIS image before and after atmospheric correction.

HESSD
6, 7001–7024, 2009

Fig. 10. LAI map retrieved using DSD method.

HESSD
6, 7001–7024, 2009

Fig. 11. LAI map retrieved using empirical relationship between LAI and NDVI.

HESSD
6, 7001–7024, 2009